Holographic Optical Element for LIDAR scanning systems

Ashkan Arianpour[a], Graham Nelson[a], Tim Christianson[a], William Clifton[b]
[a]Quartus Engineering, Inc. 9689 Towne Centre Drive San Diego, 92131
[b]L3HARRIS 1025 W. NASA Boulevard Melbourne, FL 32919

ABSTRACT

Airborne LIDAR sensors can produce accurate 3D point clouds for terrain mapping at different altitudes. As the altitude increases, there is a need for larger aperture sizes to ensure the collection of sufficient photons and the preservation of spatial resolution. In the case of conical scanning optical systems, axially spinning refractive wedges can be used to cover a scan across the field of regard. Nevertheless, maintaining rotational balance for refractive wedges proves challenging, particularly at angles exceeding several degrees, due to their asymmetric moment of inertia. In contrast, a holographic optical element serves as an alternative scanning optic with a symmetric moment of inertia, effectively addressing stability concerns associated with substantial scan angles compared to refractive wedge-based scanners. Our study highlights that HOEs can accommodate a wide range of scan angles and aperture sizes without compromising volumetric constraints or stability, showcasing their effectiveness in optical scanning for LIDAR sensors.

Keywords: Diffractive optics, holographic optical elements, LIDAR, scanning

1. INTRODUCTION

LIDAR (Light Detection and Ranging) scanning systems are known for providing detailed and accurate 3-dimensional point clouds, generating precise terrain mapping and modeling[1]. The increasing demand for operations at higher altitudes necessitates scaling aperture sizes to achieve their photon budget—essentially receiving enough photons to satisfy a Signal-to-Noise Ratio (SNR) associated with a targeted spatial resolution. An architectural trade-off exists regarding the location of the scanning mechanism. Placing the scanner in the front of a system simplifies the collection optics but results in a larger scanning optical component to match the clear aperture of the optical system. Conversely, positioning the scanner downstream of the optical train can reduce the size of the scanning component, but can result in more complex optics to accommodate the broader field angle.

The integration of a front-end refractive wedge-based scanner offers a streamlined optical scanning system aligned with the rest of the optics. However, as scan angle requirements increase, so does the necessary wedge angle, resulting in the rotational stability of the refractive scanner being compromised due to the asymmetry of the optic. While a counterbalance on the thinner side of the wedge partially mitigates this asymmetry, at large diameters the asymmetric moment of inertia becomes more difficult to stabilize and can induce a significant amount of stress in the refractive optic (Figure 1), limiting the operational scan speed. As an alternative, a diffractive optic in the form of a holographic optical element (HOE) can be substituted as the scanning component[2]. A holographic optical element can be characterized by an oscillation in refractive index, inducing a phase variation that enables an efficient diffracted beam at a determined angle. In response to the challenges associated with refractive wedge-based scanners, we explore the fabrication and effectiveness of a holographic optical element for a Geiger-mode LIDAR sensor demonstrating a symmetric moment of intertia for a range of scan angles.

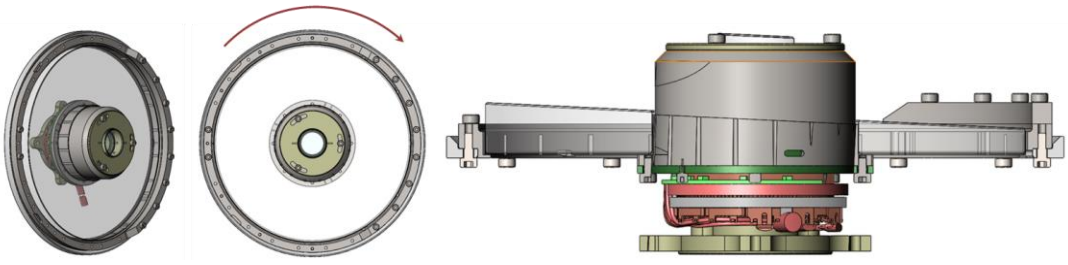

Figure 1. Isometric, top, and side views of a refractive spinning wedge for a 2° scan angle with an asymmetric moment of intertia.

Photonic Instrumentation Engineering XI, edited by Lynda E. Busse, Yakov Soskind, Proc. of SPIE Vol. 12893, 1289304 · © 2024 SPIE
0277-786X · doi: 10.1117/12.3001142

2. LIDAR SCANNING ARCHITECTURE

2.1 LIDAR Optical System

The required clear aperture for the HOE was set to match the entrance aperture of the LIDAR sensor's receive path (253mm outer diameter with a 110mm inner diameter). The HOE would be positioned in front of an 1400mm focal length RC telescope with a Geiger-mode sensor as the focal plane array. The LIDAR sensor utilizes a canonical scan where time of flight measurements are conducted in the direction of travel gathering information ahead and behind of the aircraft. The scanner is aligned with the optical axis of the LIDAR sensor, making a transmission hologram the preferred choice for our scanning mechanism (Figure 2). The LIDAR sensor has two main optical paths: a transmit path (Tx) and receive path (Rx). The transmit path passes through the center of the scanning mechanism through a 1" wedge prism with a 15° deflection angle. This optic is rather small and has an insignificant contribution to the overall balance of the scanner. The Tx and Rx scanners deflection angles are rotational offset to compensate for the difference in time of flight between the transmitted light reaching the ground and the return beam reaching the receiver.

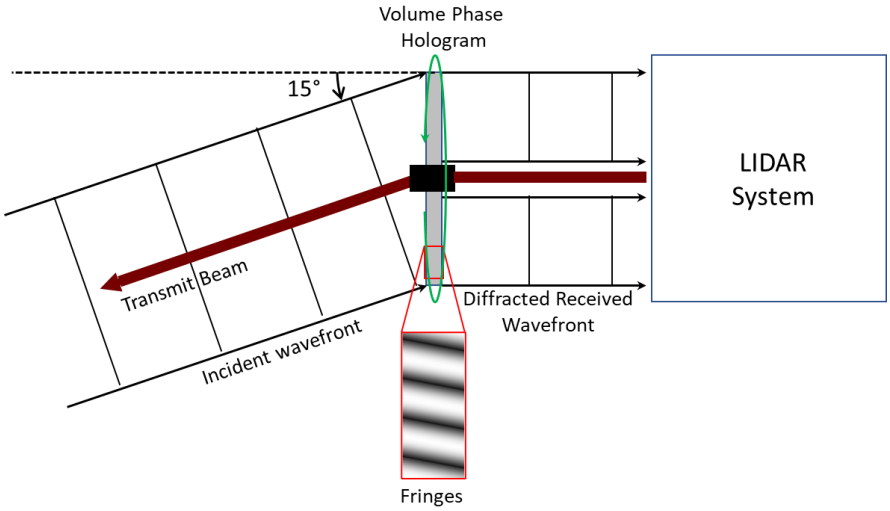

Figure 2. Diagram of the proposed holographic optical element receive scanner in line with a LIDAR system.

2.2 Holographic Optical Element Recording

The fabrication of the hologram was completed by interfering two angularly separated beams illuminating a surface to produce a constant linear fringe pattern. The orientation and periodicity of the fringes is determined by the angles of incidence and wavelength of the source. A nearly 4µm fringe period is required to achieve the 15° diffraction angle at the operating wavelength of 1064nm. However, recording a hologram in the infrared spectrum poses challenges due to the inability to visually perceive the light and limitations in the film's photosensitivity. To overcome these challenges, we used a 1W Cobolt 532nm laser to achieve the power density required to record the fringe pattern, while providing the visual feedback easing the alignment process. The coherence length of the laser far exceeded the difference between path lengths as well. Adjusting the power between each of the channels, we optimized the uniformity and maximized the fringe contrast. The final collimation of the beam was achieved using 300mm diameter off-axis parabolic mirrors, adjusting the slant angle proportionally to the change in wavelength between 532nm and 1064nm wavelengths. Figure 3 shows the layout of the optical set up. Wavefront quality was assessed by independently evaluating each beam interferometrically to reduce low-order aberrations such as power, astigmatism, and coma.

The recording medium was a Bayer Hx 24µm holographic film that was photosensitive in the visible spectrum[3,4] and could still provide an adequate modulation depth to achieve a high diffraction efficiency at 1064nm. The film was applied to a fused silica glass surface and laser cut to the shape of the entrance aperture of the LIDAR system. Each recording took approximately 40-60sec of exposure time. This extended period of exposure is primarily a result of

twofold: 1) expanding the beam to an aperture of 300mm results in a lower power density, and 2) a significant amount of light is omitted by cropping the center of the gaussian beam to generate a uniform intensity across the target. A fringe locker comprised of a mirror axially pistoning based on fringes position was also integrated into one of the channels of the optical setup. The fringe locker's main function was to compensate for the variation in optical path length between the two arms of the setup caused by difference in atmospheric scintillation. Albeit the fringe locker is only able to measure a subsection of the beam due to its limited sensor area.

Polymerization of monomers occurs in bright areas in response to the two beams of light interfering, leading to a sinusoidal oscillation in refractive index throughout the film.[3,4] This fluctuating index of refraction represents the phase modulation of the hologram, and ultimately determines the efficiency of the diffracted beam. Following the completion of recording, a settling period is advisable to allow for polymer diffusion, moving away from dark areas and toward bright regions. Finally, the film requires a post-process referred to as bleaching whereby an additional illumination step is applied with multispectral light spanning from visible to UV, fixing the recorded interference pattern. After recording the HOE, we affixed a second fused silica optic onto its surface, creating a sandwich structure and sealing the HOE from the environment using a UV epoxy (MasterBond UV15) with a refractive index similar to that of the holographic film. Due to the extensive bond area, shrinkage of the epoxy resulted in a slight warping of the optic and caused the transmitted wavefront error to grossly exceed the requirement. To address this, a crucial post-processing step involved double-side polishing the bonded HOE to flatten both exterior surfaces and reduce the warped figure of the optic.

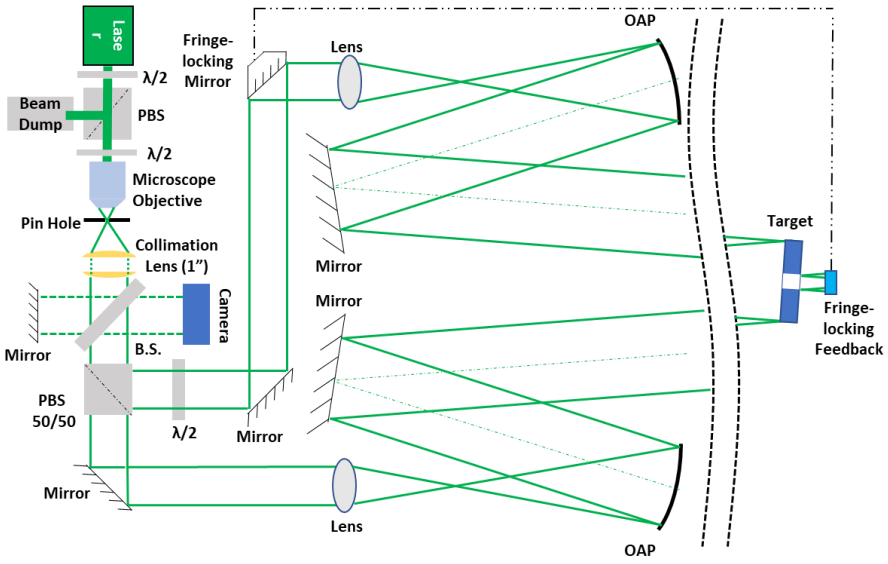

Figure 3. Diagram of lab setup for recording a holographic optical element.

3. LIDAR PERFORMANCE

3.1 Holographic Optical Element Performance

Based on the wavefront budget of our LIDAR sensor, the HOE was specified to achieve a wavefront error of λ/8 RMS at 1064nm, and a 1st order diffraction efficiency of 65%. Validation of the HOE's post-processing performance involved measuring the wavefront error of the 1st order diffraction beam using a Zygo interferometer at 633nm. Despite observing some discontinuities, the diffraction efficiency at 633nm was sufficient to measure the transmitted wave's performance (Figure 4). Scaling for our wavelength of operation (1064nm), we achieved an RMS wavefront error of λ/12.7 over 90% of the clear aperture after subtracting the defocus term. Our alignment process allowed the adjustment of the focal plane's position such that the amount of defocus from the HOE can be subsumed into the overall focal length. Using a 1064nm light source and averaging over sub-apertures extensively throughout the HOE, we achieved an average diffraction efficiency of nearly 70% across the clear aperture.

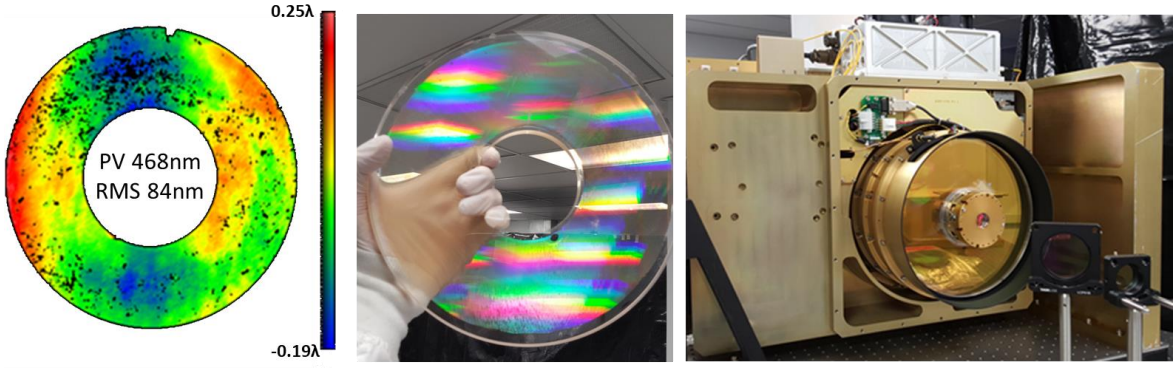

Figure 4. Left) Double-pass measurement of 1st order wavefront error through a Zygo Interferometer scaled for 1064nm with defocus removed; Middle) Photo of a bonded holographic optical element displaying diffractive properties; Right) LIDAR sensor integrated with the HOE.

3.2 LIDAR Sensor Performance

The LIDAR system's image quality hinged on the ensquared energy of the point spread function (PSF) as measured on the detector. Projecting the Tx laser source as a point source and collimating it into the receive path, we quantified the expected optical performance of the LIDAR's receive path through the HOE. Prior to integrating the HOE, the maximum ensquared energy of the receive telescope was 83% on a single pixel. Following the HOE's integration, the maximum ensquared energy dropped to 50% on a single pixel. The drop in optical performance can be attributed to the diffractive properties of the hologram causing the 0.3nm linewidth of the laser to spread across the PSF as depicted in Figure 5. The fringe pattern of the HOE only varies in one direction and so the spread of the spectral content will rotate as the HOE scans.

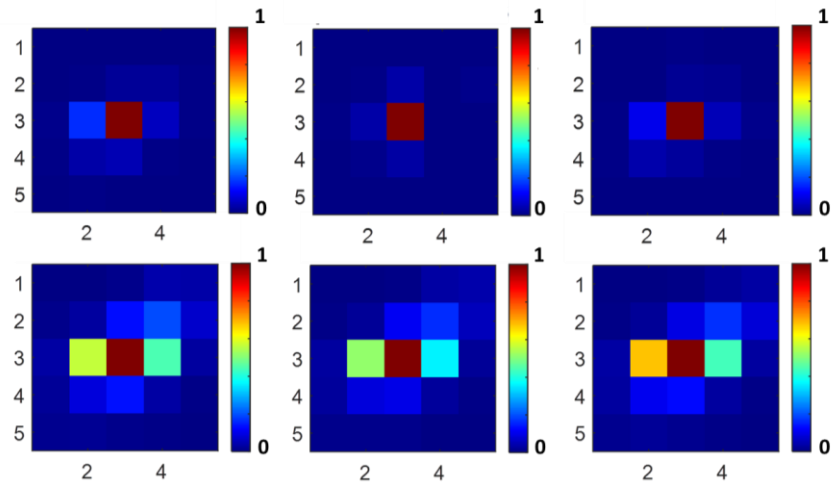

Figure 5. Top row) Several PSFs taken at different parts of the focal plane array of the receive path without the HOE installed; Bottom row) Same as top row with the addition of the HOE installed into the scanner. The spread of the laser's linewidth can be seen on the PSF in one direction.

Operational performance of the LIDAR system was evaluated by capturing a 3D point cloud of the terrain during an operational scan and flight path, utilizing an aircraft carrying the payload to 13,000 feet while operating the scanner at approximately 1400rpm. It is noteworthy that VeriDaaS is now the owner of the LIDAR sensor, and they have provided the images in Figure 6 showing a relative colormap depicting the differences in height of the measured terrain. With the conical scan and the fully integrated HOE, the LIDAR sensor demonstrated a lateral spatial resolution up to 50 points-per-meter and a vertical resolution of 10cm.

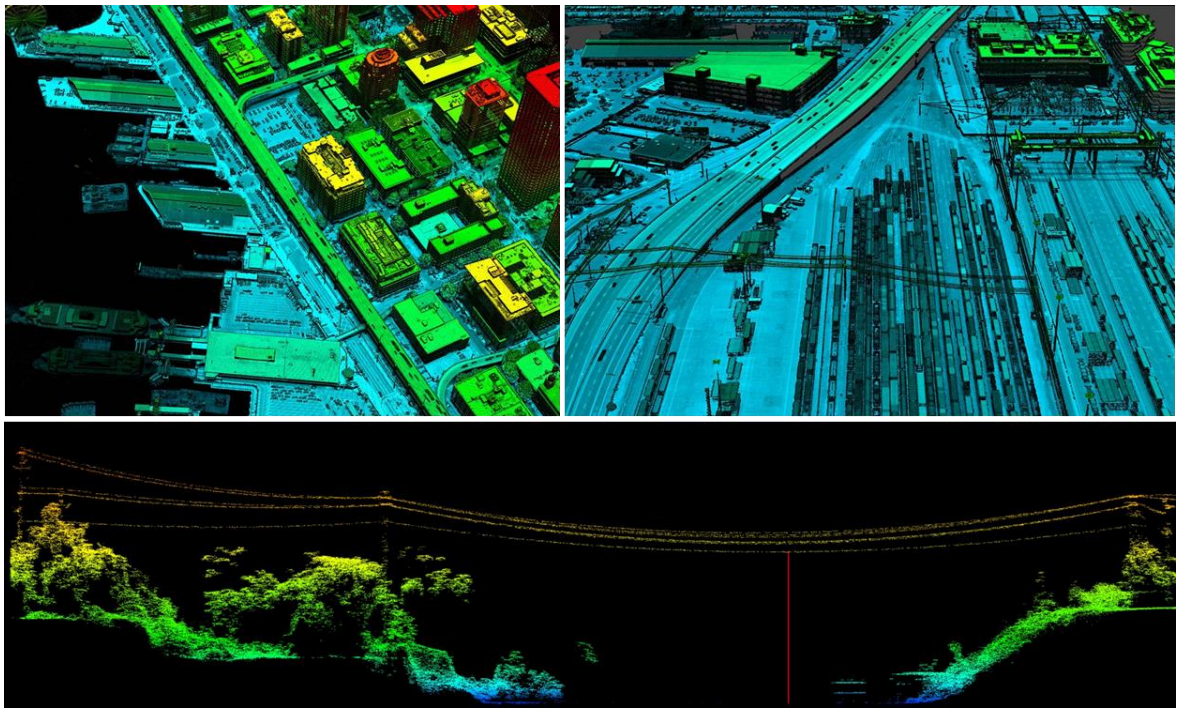

Figure 6. 3D point clouds generated by the HOE scanning LIDAR at an altitude of 13,000ft.

4. CONCLUSION

We have successfully showcased the recording of a large holographic optical element designed for a conical scanning LIDAR sensor. The entire process, encompassing recording, bonding, and post-processing of the HOE, resulted in a wavefront error and diffraction efficiency that aligned with our specified criteria. We observed that after installing the HOE, the spectral linewidth of the laser diffracted, causing a 1-dimensional spread of the PSF. However, future systems could mitigate this spread with a narrower linewidth transmission source. While our deflection angle was only 15° for this system, the HOE would be capable of much larger angles with virtually no change to its physical mass or volume. The ultimate performance of the scans produced high-quality image data suitable for supplying end-users with the necessary information to capture the three-dimensional properties of the terrain. Three HOE scanners have been fabricated and integrated onto their respective LIDAR sensor and have been operational for several years.

We would like to also acknowledge Cameryn Yow and Michael Ricci for their relentless support for developing this system and VeriDaaS for providing the LIDAR image data for this publication.

REFERENCES

[1] R. T. H. Collis, "Lidar," Appl. Opt. 9, 1782-1788 (1970)
[2] Schwemmer, G., Rallison, R., Wilkerson, T., and Guerra, D., “Holographic optical elements as scanning lidar telescopes,” Optics and Lasers in Engineering, Volume 44, Issue 9, 2006,
[3] Berneth, H., Bruder, F. K., Fäcke, T., Hagen, R., Hönel, D., Jurbergs, D., Rölle, T., and Weiser, M. S., "Holographic recording aspects of high-resolution Bayfol HX photopolymer," Proc. SPIE 7957, Practical Holography XXV: Materials and Applications, 2011.
[4] Berneth, H., Bruder, F. K., Fäcke, T., Jurbergs, D., Hagen, R., Hönel, D., Rölle, T., Walze, G., "Bayfol HX photopolymer for full-color transmission volume Bragg gratings," Proc. SPIE 9006, Practical Holography XXVIII: Materials and Applications, 2014